DEVELOPMENT OF ESTIMATION FOR POTENTIAL SOLAR ENERGY USING DSM DATA

Sung-Jae Kim[1] · Kwang-Deuk Kim[2] · Chang-Yeol Yun[2] · Myung-Hee Jo[3]

[1] Institute of Spatial Information Technology Research, GEO C&I Co., Ltd, Sungjaekim97@hanmail.net
[2] Dept. of Renewable Energy Research, Korea Institute of Energy Research, kdkim@kier.re.kr, yuncy@kier.re.kr
[3] Dept. of Satellite Geoinformatics Engineering, Kyungil University Korea, mhjo@kiu.ac.kr

KEY WORDS: Renewable Energy, LiDAR, solar energy resource amount, grade map

Abstract: In the recent years of global warming, there has been increasing interest in new regenerative energy reserves as regards resolving the global environmental problems and securing the eco-friendly energy resources in terms of constructing a global environmental recycling society. In order to tap the recently highlighted spatial information technology and its usability for solar energy, a new regenerative energy, this research produced a solar energy reserve grade map utilizing the digital surface model (DSM) data based on LiDAR (Light Detection and Ranging). The selected target site was Uleung-do, Uleung-gun located in Gyeongsangbuk-do. Through the new LiDAR photography and data processing on the whole area of Uleung-gun was created a 1m contour, which was utilized for constructing the 1m DSM data. The DSM data was utilized for identifying the incidence range of solar rays by solar altitude and azimuth and for the solar energy reserve assessment technology; solar energy reserve grade mapping based on the precise and accurate 1m spatial resolution of data is expected to be able to reflect more accurate information and suggest the scientific and rational method to assess the new regenerative energy reserve.

INTRODUCTION

For all global economic crises at present, bold investment is progressing in the new regenerative energy sector, particularly in the solar energy market which is playing a key role of the new-generative-energy green industry as shown in the average annual growth amounting to 80% through 2010. Besides, much interest is in developing the management system based on the actual reserve of new generative energies, with much amount of cost and labor in the annually produced national energy management system and energy reserve assessment in connection with spatial information technology. To acquire the stability of these new regenerative energy resources, the energy reserve assessment should be conducted necessarily, and among the various new regenerative energy sources, particularly solar energy is being actively researched with GIS analysis technique in and out of country. The recent improvement of accuracy and precision in spatial resolution such as three-dimensional GIS, high-resolution satellite imaging, aerial photography, and LiDAR along with the NGIS project (e.g. production of 1:1,000 digital maps) is utilized in the new regenerative energy sector based on a variety of approaches.

This research aimed at utilizing LiDAR data which enables quick and objective spatial data acquirement, research time saving, possible cost-saving measures, and the quick and easy analysis of broad areas, as well as quick identification of the overall condition of geographic information in conducting GIS analysis such as grade classification through overlaying and error index analyses, and thus producing the solar energy reserve grade map. This enabled more accurate and systematic preparation of research framework for utilizing GIS in the solar energy sector.

RESEARCH DATA AND METHODS

The selected target area was Uleung-gun, Gyeongsangbuk-do, located at the longitude of 130°48′-131°52′E and the latitude of 37°14′-37°33′N. Except Uleung-do isolated on the East Sea, its attached islands such as Gwaneum-do, Juk-do, and Dok-do, and such rock islands as Samseon-am, Gong-am, Juk-am, Cheong-do, Bukjeo-am, and Chokdae-am were excluded from the target sites of this research. The Uleung-do island as the target site occupies 98% of the whole area of Uleung-gun. For the solar energy reserve grade mapping, the LiDAR data acquired from

new aerial photography was utilized and constructed. The photography was conducted four times for three days from June 4 to 6 in 2011, utilizing such LiDAR survey apparatus as the Canadian company Optech's ALTM 30/70 model. This apparatus shows 70 kHz as the maximum laser pulse scanning rate, can be operated up to the altitude 3,000m, and its laser point density can acquire more than 2-3 points per 1m unit area. For the 1m contour and DSM data construction, TerraScan software was utilized; for the reserve assessment analysis, the Spatial Analysis tool of ArcGIS 9.2 software was utilized.

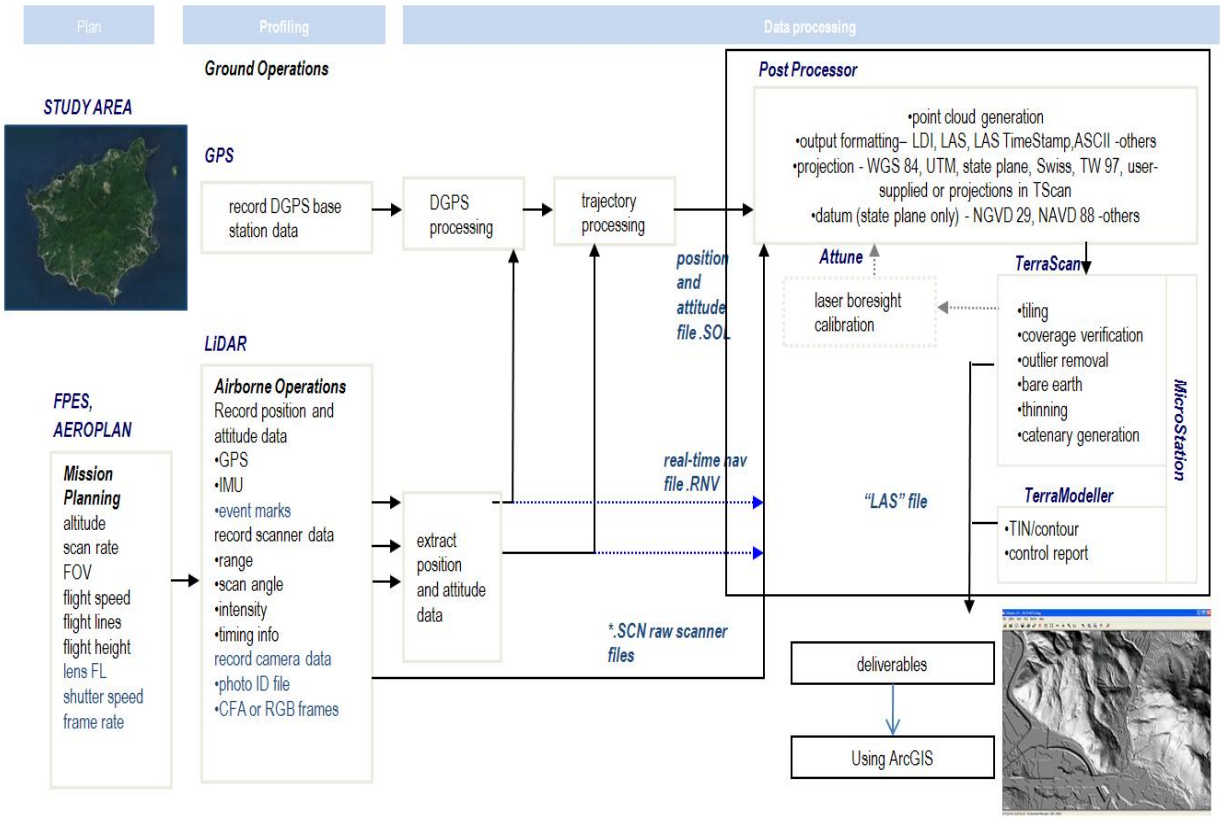

Figure 1: The Study Area and Flow Chart

RESULTS & DISCUSSION

LiDAR Survey for 1M DSM Data Construction

For construction of the 1m precision DSM data to be used in this research, a new LiDAR survey was conducted. This LiDAR survey refers to the method of surveying in sequence like figuring out with GPS the three-dimensional position of a laser scanner that emits a laser pulse, measuring the time and intensity taken for the return of the projected scanner, process the measured data in combination with the positional information recorded in the INS mounted on the scanner from the time of projection, and thus measure the accurate three-dimensional position of the reflector (Ministry of Land, Transportation, and Maritime Affairs, 2006). The acquired data from LiDAR survey was converted from the compressed data at the time of initial photography through a pre-process to the usable form of point data. Also, the inherent errors of the aerial survey apparatus were determined and the generated errors were corrected through calibrations in this research, territorial and aerial calibrations. The correction of system errors were conducted on the calibration factors shown in table 1.

Table 1. Calibration Factor

Calibration Factor	Contents
Roll	- Aerial of the X-axis of rotation error calibration
Pitch	- Aerial of the Y-axis of rotation error calibration
Heading	- Aerial of the Z-axis of rotation error calibration
Range	- Calibration of the distance deviation on aerial surveying equipment
	- Aerial laser Survey Results and Ground Control Point Using in the Testing Sites for Calibration
	- Periodic calibration on the changes in value and time difference
Torsion	- calibration on physical constant on system scanning mirror
	- the scan angle calibration influence
	- Periodic calibration on the changes in value and time difference

Development of DSM-based Solar Energy Reserve Assessment Technique

1. Information Analysis of Solar Azimuth and Altitude

To estimate the incidence area of solar rays in the research target area, Uleung-gun was selected as the representative area. For this area, the monthly average solar azimuths and altitudes from January to December in 2010 were calculated. The solar azimuth corresponds to the angular distance between the intersections with the meridian and with the azimuth on the horizon. Also, the solar azimuth is generally displayed by the angle deviated from the frontage such as S-30°-E and S-40°-W. The solar altitude refers to the angular distance between the solar rays and the horizon, as one of the coordinates displaying the solar position. When referring to the solar declination (displaying the complementary angle of the angle between the directions of the solar rays and the North Pole) as δ, the latitude on the earth as φ, the zenith distance (displaying the complementary angle of the angular distance or altitude measured from the observer's zenith through the meridian to the celestial body) as z, the solar altitude as h, and the solar hour angle as t, their relation can be expressed as follows:

$$\cos z = \sin\varphi\sin\delta+\cos\varphi\cos\delta\cos t,\ h= 90°- z.$$

For calculation of the average, the hourly longitude-latitude coordinates, altitudes, right ascensions, and declinations were calculated above all into the daily averages, which were recalculated into the monthly averages. TABLE 2 shows the hourly azimuths, altitudes, right ascension, and declinations at the target site [Lat./Lng.: (37.49255400286561, 130.8943998474122)] from January 1 to December 31 in 2010. Meanwhile, the nighttime data with negative altitude reflecting no solar incidence were not included in calculating the average.

Table 2. Calculation of the average daily values of solar altitude and azimuth

Time	Azimuth			Elevation			Right ascension			Declination		
	Degree	Minute	Second	Degree	Minute	Second	Degree	Minute	Second	Degree	Minute	Second
00:00	355	40	42.90	-75	09	34.5	16	26	10.70	-21	41	20.2
01:00	040	43	55.00	-70	15	02.3	16	26	21.60	-21	41	44.3

02:00	065	36	12.60	-60	38	25.4	16	26	32.50	-21	42	08.4
03:00	076	49	43.20	-49	16	50.8	16	26	43.37	-21	42	32.7
04:00	089	59	44.30	-37	26	40.8	16	26	34.23	-21	42	57.0
05:00	098	36	48.20	-25	35	44.0	16	27	05.05	-21	43	21.4
06:00	106	50	01.40	-14	00	10.3	16	27	15.85	-21	43	45.7
07:00	115	21	39.40	-2	54	44.3	16	27	26.61	-21	44	10.0
08:00	124	45	33.60	07	22	47.6	16	27	37.34	-21	44	34.2
09:00	135	32	56.80	16	28	26.7	16	27	48.04	-21	44	58.3
10:00	148	09	23.80	23	49	48.0	16	27	58.71	-21	45	22.3
11:00	162	41	07.40	28	47	17.0	16	28	00.37	-21	45	46.1
12:00	178	34	48.00	30	43	34.7	16	28	20.02	-21	46	09.8
13:00	194	35	45.90	29	20	55.5	16	28	30.67	-21	46	35.2
14:00	209	25	06.40	24	52	09.3	16	28	41.33	-21	46	36.5
15:00	222	21	29.60	17	52	32.1	16	28	52.01	-21	47	19.6
16:00	233	25	42.10	09	02	12.5	16	29	02.71	-21	47	42.6
17:00	243	01	14.80	-1	04	56.4	16	29	13.45	-21	48	05.5
18:00	251	28	47.10	-12	03	36.7	16	29	24.21	-21	48	28.3
19:00	259	51	25.40	-23	35	12.9	16	29	35.02	-21	48	51.0
20:00	268	18	56.00	-35	24	48.5	16	29	45.86	-21	49	13.7
21:00	278	036	04.60	-47	17	03.9	16	29	56.73	-21	49	36.5
22:00	291	12	26.00	-58	47	52.3	16	30	07.63	-21	49	59.3
23:00	313	22	08.50	-68	55	30.3	16	30	18.54	-21	50	22.2

2. Numerical Overlay Analysis for Solar Energy Reserve Grading

The average azimuths and altitudes recalculated as the monthly average in the analysis of solar azimuth and altitude information were input to the Arc GIS and the monthly hillshades were drawn up. The hillshade is a map to effectively display the shade by the geographic altitude, and the map constructed in this study has 8 bit (0-255): the value closer to 255 means brighter area, which means relatively higher incidence of solar rays. Twelve hillshades on Uleung-do from January to December were created (Figure 4). For solar energy resource grading based on the created twelve hillshades, numerical overlay was utilized to create a layer that shows the summed values of all the layers. As a kind of drawing overlay techniques, the numerical overlay gives numeric points on drawings instead of mapping colors or shades, and this research adopted ordinal combination method.

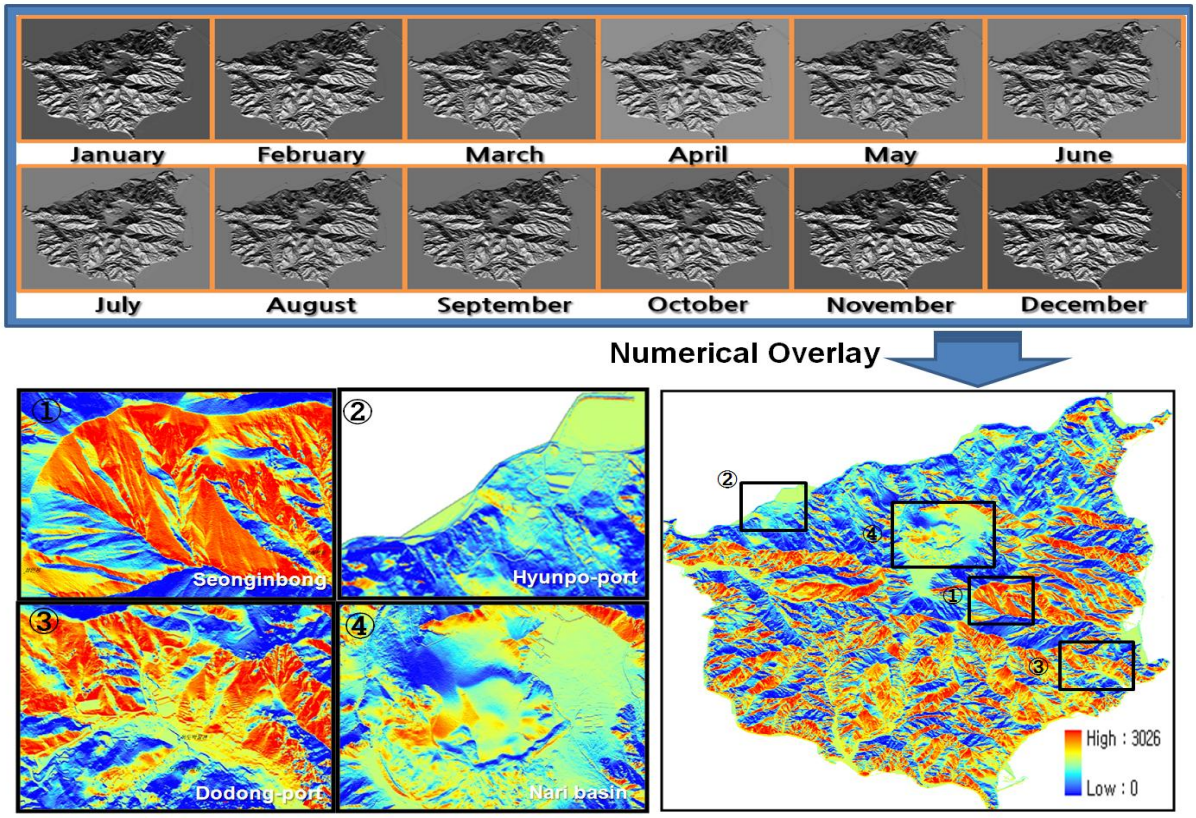

Figure 2. Production of solar energy resource grade mapping using Numerical Overlay Analysis

3. Solar Energy Reserve Grade Mapping

The solar energy reserve values acquired from the numerical overlay are relative values that have the wide range from 0 to 3026. The wide-ranging values have an advantage in providing detailed information, but also have difficulties in providing decision-making, fusing with relevant data, or utilizing the data. To make up for these disadvantages, the grade map that divided the solar energy reserve values into grade sections was created. This research classified the values into ten grades based on the five kinds of grade classification including the individual descriptive classifications which can be embodied by ArcGIS (an IS analysis tool) such as natural breaks and quantile, and the continuous classifications such as equal interval, standard deviation, and geometrical interval. To determine the efficiency of the used classification technique, the error index measurement technique developed by Jenks and Caspell (1971) was conducted as shown in the following equation:

$$Error\,Index\,(E) = \frac{Errors\,by\,Specific\,Classification}{Maximum\,Errors}$$

$$= \frac{Area\,Ratio\,by\,Areas \times (Median\,of\,Class\,Sections - Actual\,Observation)^2}{Area\,Ratio\,by\,Areas \times (Median\,of\,Class\,Sections - Mean)^2}$$

The closer the error index value to 1, the lesser error it means. Table 3 shows the error index about natural breaks, equal interval, geometrical interval, standard deviation, and quantile.

Table 3. Error index calculated according to the classification

classification	Natural breaks	Equal interval	Geometrical interval	Standard deviation	Quantile
According to the classification error	0.854	1.241	1.201	0.889	1.283
error index	0.845	0.814	0.867	0.839	0.827

As a consequence of looking into the error index about each grade classification, there appeared the least error in the geometrical interval. Thus, this research drew up the solar energy reserve grade map utilizing the geometrical interval, which means the closer to Grade 10; the relatively more sunlight enters into the area. The map was constructed not only to the 1m, but also to a 500m spatial resolution for efficient analysis and use.

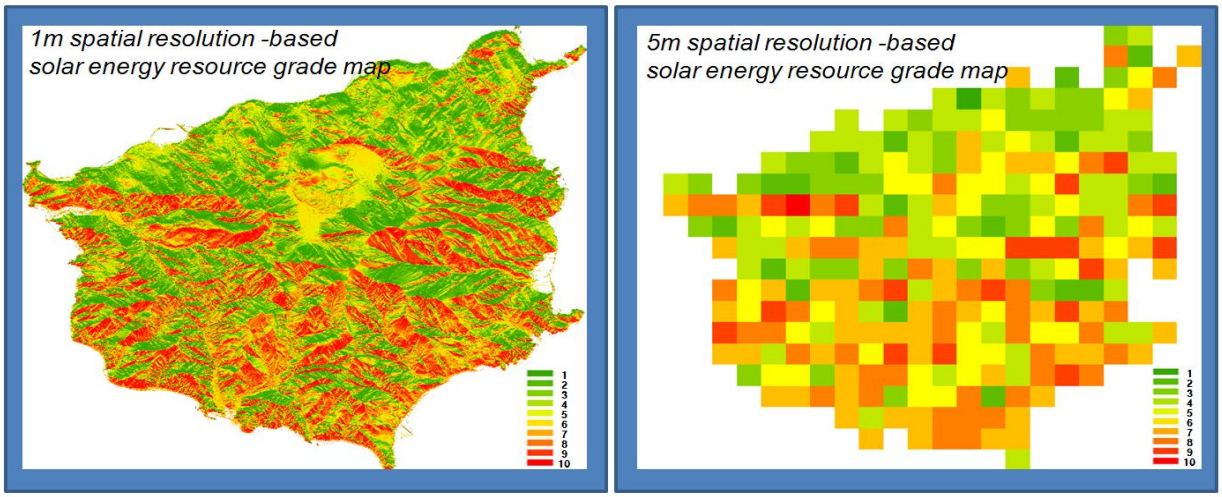

Figure 3. 1m/5m spatial resolution - based solar energy resource grade map

CONCLUSIONS & RECOMMENDATIONS

This research produced a solar energy reserve grade map in order to tap the recently highlighted spatial information technology and its usability for solar energy. For this purpose, it pre-processed and post-processed the LiDAR-based data, and on this basis constructed 1m DSM. Figuring out the incidence range of solar rays by the DSM data, solar altitudes and azimuths, it utilized the monthly average data in calculating the hillshade. After deriving the total numerical points of relative hillshade values by months, it analyzed grade classification errors and drew up the solar energy reserve grade map.

1. By utilizing the LiDAR data - which had been mainly utilized for spatial information (e.g. numerical map, three-dimensional geography production, and survey) and other new generative energies (forest biomass) for solar energy, it prepared the GIS-based research framework for solar energy with more accurate information, as well as tapping the usability for such new regenerative energies as wind power and small hydro power that can employ geographic information.

2. Amongst the analysis of grade classification error index conducted in this research, the best result appeared in the geometrical interval. This result is somewhat different from the existing analysis of GIS grade classification error index (the natural breaks showed the least errors where there had not much uneven geography; see National Disaster Management Institute, 2011 & Yeo, C.G., 2011), and considered the result of much uneven geography on Uleung-do (large variation of geographic altitudes). This seems the case of a good classification method that can easily applied to the geographic values that show many accumulative figures of geometric progression.

3. The most ideal assessment technique is to evaluate the reserve in a detailed unit like kW, but this kind of technique involves many variables to consider and is limited to be expressed and analyzed by a GIS analysis technique. Thus, this research produced the grade map focusing on the relative analysis method for the solar energy reserve assessment. This solar energy reserve grade map is expected to provide information for supporting rational decision-making in the suitable-land analysis, quantitative information collection, management, and analysis for a solar energy building.

It is expected in future that not only the geometrical characteristics, but also other solar-energy-related data such as those from field observation and weather survey will be fused with each other so as to enable more accurate solar energy reserve assessment and grade mapping, accordingly calculating the amount of electric power generation and implementing economic assessment, ultimately serving as a basic data to be utilized for analyzing the domestic energy demands/supplies and planning the overall national energy policies.

REFERENCES:

National Disaster Management Institute (2011). Disaster Geographic Information System Operating System Construction Report. pp.90-91.

National Geographic Information Institute (2007). Multi-Dimensional Spatial Information Construction Technical Service Report. pp.39-49.

Ministry of Land, Transportation and Maritime Affairs (2006). Efficient Construction, Modification, and Revision of NGIS DB Using LiDAR. pp.9-10.

Korea Institute of Energy Research (2011). Three-Dimensional Spatial-Information-based New Regenerative Energy Field Assessment System Development Report. pp.1-2.

National Disaster Management Institute (2011). Disaster Geographic Information System Operating System Construction Report. pp.90-91.

National Geographic Information Institute (2007). Multi-Dimensional Spatial Information Construction Technical Service Report. pp.39-49.

Ministry of Land, Transportation and Maritime Affairs (2006). Efficient Construction, Modification, and Revision of NGIS DB Using LiDAR. pp.9-10.

Korea Institute of Energy Research (2011). Three-Dimensional Spatial-Information-based New Regenerative Energy Field Assessment System Development Report. pp.1-2.